

RESEARCH

Open Access



Comprehensive comparative analysis of infrapatellar fat pad morphologies in a longitudinal knee osteoarthritis exploratory study: new insights into its role as an independent prognostic marker

Jean-Pierre Pelletier^{1*} , Patrice Paiement¹, François Abram¹, Marc Dorais², Jean-Pierre Raynaud¹ and Johanne Martel-Pelletier¹ 

Abstract

Background No established markers can effectively phenotype knee osteoarthritis (OA) patients into subgroups. Infrapatellar fat pad (IPFP) morphology data that can forecast disease symptoms, structural changes, and knee replacement (KR) are sparse and conflicting. This 96-month longitudinal exploratory study aimed to identify which IPFP morphological features were the most effective independent prognostic markers against these outcomes.

Methods This longitudinal study analyzed 1075 target knees (one knee per participant) from the Osteoarthritis Initiative (OAI) progression cohort. Structural changes include cartilage, bone marrow lesions (BMLs), and joint effusion volumes assessed using automated and quantitative magnetic resonance imaging systems (MRI). The IPFP global and signal (hyper- and hypo-) intensity volumes and areas were assessed using MRI combined with a newly developed, fully automated neuron-driven technology.

Symptoms were evaluated using WOMAC scores. Data on KR was obtained from the OAI database. Data were collected at baseline and 12, 24, 48 and 96 months and analyzed using a mixed model for repeated measures (MMRM) or ANCOVA.

Results The baseline characteristics were mild to moderate knee OA. Over time, disease symptoms (WOMAC), cartilage volume, IPFP global and hypointense signal volumes, and maximal and hypointense signal areas decreased (all $p \leq 0.001$). Joint effusion and hyperintense signal volume and area increased (both $p \leq 0.001$).

Associations were found between IPFP morphologies at inclusion and changes in cartilage volume (hypointense and hyperintense volumes, 48, 96 months, $p \leq 0.04$), BML volume (global volume 48 months, $p = 0.05$; hyperintense area, 12 months, $p \leq 0.04$), and effusion volume (hypointense volume 48 months and hyperintense volume 96 months, $p \leq 0.05$).

At inclusion, smaller IPFP sizes (below median) were associated with cumulative KR at 96 months (global and hypointense volumes, $p \leq 0.04$ and maximum area, $p = 0.05$).

*Correspondence:

Jean-Pierre Pelletier

dr@jppelletier.ca

Full list of author information is available at the end of the article



© The Author(s) 2025. **Open Access** This article is licensed under a Creative Commons Attribution-NonCommercial-NoDerivatives 4.0 International License, which permits any non-commercial use, sharing, distribution and reproduction in any medium or format, as long as you give appropriate credit to the original author(s) and the source, provide a link to the Creative Commons licence, and indicate if you modified the licensed material. You do not have permission under this licence to share adapted material derived from this article or parts of it. The images or other third party material in this article are included in the article's Creative Commons licence, unless indicated otherwise in a credit line to the material. If material is not included in the article's Creative Commons licence and your intended use is not permitted by statutory regulation or exceeds the permitted use, you will need to obtain permission directly from the copyright holder. To view a copy of this licence, visit <http://creativecommons.org/licenses/by-nc-nd/4.0/>.

Conclusion This longitudinal exploratory study, leveraging a fully automated technology, highlights that i) IPFP volume (global and both signals) is superior to area metrics in predicting long-term structural changes in OA, and ii) smaller IPFP volume and area are linked with reduced need for KR. These findings provide new insights into the usefulness of IPFP morphology as a predictive biomarker of knee OA outcomes, offering a new approach to stratifying knee OA patients.

Keywords Longitudinal study, Infrapatellar fat pad, Knee osteoarthritis, Magnetic resonance imaging, Infrapatellar fat pad, Outcome, Knee replacement

Introduction

Knee osteoarthritis (OA) is a complex chronic articular disease that affects all joint tissues, leading to impaired mobility and diminished quality of life. Given the multifactorial nature of OA, early diagnosis and an effective prognostication remain challenging yet important for disease management and improving patient outcomes.

In recent years, of the work done on studying OA markers [1], there has been a growing interest in the infrapatellar fat pad (IPFP) as a potential biomarker and prognostic marker for knee OA [2, 3]. IPFP, located within the anterior knee compartment, is a large, intracapsular, and extra synovial structure rich in blood vessels, nerves, and inflammatory cells. It plays a complex role in knee joint physiology/pathophysiology, contributing to this tissue's biomechanics by providing cushioning, acting as a source of factors that may influence joint health, and involving the OA inflammatory processes central to this disease pathogenesis. Hence, it contributes to local inflammation within the knee joint by secreting pro-inflammatory cytokines, adipokines, chemokines, and inflammatory lipid mediators, which may exacerbate OA joint tissue degradation and contribute to pain and functional impairment [4–7].

Magnetic resonance imaging (MRI) is acknowledged as the state-of-the-art modality for evaluating IPFP morphology [3, 8]. However, in knee OA, various MRI techniques have been employed to assess IPFP alterations over time, leading to conflicting results, which could result from the lack of homogenization between studies, including the use of different knee OA populations, differing imaging acquisition protocol between studies, the use of different software and methods to assess and quantify IPFP volume, area and intensity signals [2, 3, 9–25]. Moreover, signal (hyper- and hypo-) intensity changes have been associated with the onset and progression of OA and linked with different stages and features of disease progression [13, 19, 24]. Some studies indicate that the enlargement of IPFP contributes to joint structure damage, increased knee pain and disability [2, 10, 18, 25]. Conversely, others report that a

larger IPFP protects against knee pain and cartilage loss [2, 26]. Moreover, hyperintense signal changes have been proposed as a surrogate for synovitis [27, 28], whereas hypointense signals with fibrosis [29]. There is still uncertainty regarding which IPFP morphology is the best independent prognostic biomarker for OA.

While some studies reported a positive correlation between IPFP abnormalities and OA severity, others found no significant associations or suggested that the relationship was confounded by factors such as body mass index (BMI), age, and comorbidities [15, 30]. Regardless of the alterations, the relationship between IPFP morphological findings and OA symptoms, joint structural alterations and long-term outcomes remain unclear and poorly understood. This highlights the need for longitudinal studies that directly compare various IPFP morphologies to better elucidate their predictive value in OA progression and determine whether and which of its morphological characteristics can reliably predict clinical outcomes.

The objective of this exploratory study is to evaluate the predictive value of different IPFP morphologies on the long-term progression of OA. Specifically, we conducted a 96-month longitudinal assessment of IPFP features in a cohort of patients with knee OA to identify the most promising prognostic markers. Detailed morphological analysis of the IPFP was performed using MRI combined with a convolutional neural network-based segmentation [20], enabling the evaluation of various IPFP features, including volume, area, and signal intensity. The latter was assessed using a newly, fully automated software. These assessments were integrated with comprehensive evaluations of clinical symptoms, different joint tissue changes, and the knee replacement (KR) outcome. By directly comparing these IPFP features, this study aims to identify robust prognostic markers for knee OA.

The findings of this research aim to improve the understanding of how IPFP morphology influences the long-term development and progression of knee OA, which could eventually help guide the development of new targeted interventions.

Methods

This study conforms to the Strengthening the Reporting of Observation Studies in Epidemiology (STROBE) guidelines for observational studies [31].

Study design

A cohort study design was conducted to determine the most promising MRI IPFP morphology to predict the long-term progression and outcomes of knee OA.

Participants

Participants were from the Osteoarthritis Initiative (OAI) cohort (<https://nda.nih.gov/oai/>), a longitudinal study providing extensive clinical, radiological and MRI data on knee OA. This cohort comprises 4,796 participants, aged 45-79 years of both sexes, enrolled between February 2004 and May 2006 and followed for up to 108 months. The OAI cohort is divided into three sub-cohorts: Progression ($n=1,389$), Incidence ($n=3,285$) and Control ($n=122$). All participants provided written informed consent. The OAI study was conducted across four clinical sites and was approved by the Institutional Review Boards at the University of California, San Francisco (OAI Coordinating Center; Approval Number 10-00532).

Target knee

Participants in this study were selected from the OAI Progression subcohort, characterized by symptomatic radiographic knee OA (frequent knee symptoms and tibiofemoral knee osteoarthritis – Kellgren-Lawrence grades ≥ 2) at study inclusion [32]. Each participant had one designated “target knee”, which was determined based on the following criteria: i) if there was radiographic evidence of OA in only one knee, that knee was selected as the target; ii) if both knees showed signs of OA, the knee with the highest score on the Western Ontario and McMaster Universities Osteoarthritis Index (WOMAC) for pain at baseline was chosen as the target knee. MRI was performed at inclusion on the target knee for all participants. As shown in Figure 1, of the 1,389 participants (2,772 knees), 622 knees were excluded due to previous knee surgery and 1,075 knees because they were non-target knees. Thus, the final analysis included 1,075 target knees (1,075 participants), the data of which were available from study inclusion to follow-up visits up to 96 months (12, 24, 48, 96) post-inclusion.

Variables

All sociodemographic and clinical data were obtained from the OAI database (AllClinicalxx datasets),

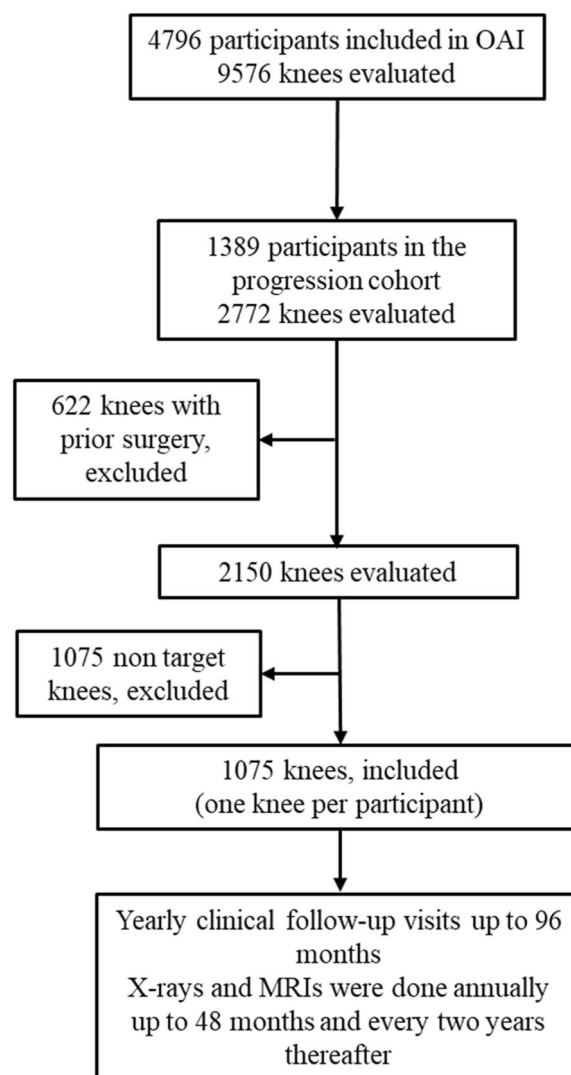


Fig 1 Flow chart of the study

including knee side, age, gender, Western Ontario and McMaster Universities Osteoarthritis Index (WOMAC) scores (total and pain) [33], body mass index (BMI), and knee arthroplasty (any partial or total KR) (V99E(R/L)KTLPR).

Changes in WOMAC scores over time were calculated as the difference between follow-up and inclusion values.

Imaging

Joint space width (JSW) at inclusion done using X-ray was obtained from the OAI database (<https://nda.nih.gov/oai/>; files: kxr_qjsw_duryeaxx).

Data for all the other tissues were analyzed using MR imaging. Scans from the OAI were performed annually for up to 48 months and biannually thereafter. MR images

were acquired from the 3.0 T apparatus (Magnetom Trio, Siemens) at the four OAI clinical centres [32].

Fully automated quantitative MRI technologies were used to assess global knee and medial compartment of cartilage and bone marrow lesions (BMLs), as well as joint effusion, utilizing a number of MRI sequences, as previously described [20, 34–36]. In brief, the sequence used for cartilage was a double echo steady state (DESS). Two sequences were used for BML: T1/T2-weighted gradient echo (DESS) and a water-sensitive intermediate-weighted turbo spin echo (IW-TSE). For joint effusion, two sequences were also used: T2-weighted gradient-echo true-fast-imaging-with-steady-state-precession sequence (T2-trueFISP) and T1-weighted inphase-outphase gradient-echo (GRE) sequences. The IPFP volume was acquired using the T2 sagittal intermediate weighted (SAG IW) 2D TSE FS sequence, as defined in the OAI protocol [32], segmented with a fully validated convolutional neural network (CNN) [20]. The IPFP hypo- and hyperintense signals used the same MRI acquisition sequence as for the volume. They were assessed using the intensities of the IPFP image in conjunction with the IPFP mask, with a signal separation method as described in Additional file 1 and Additional files 2-4, Figures S1-S3. The surface area of the 2D IPFP and the hyperintensity decomposition were calculated on the slice with the most voxels and computed by multiplying the number of voxels by the spatial resolution of the image. Cartilage was expressed as mm³, BML as a percentage of the lesion in the bone volume, effusion as mL, IPFP volume as cm³, and IPFP area as cm².

Relative changes in joint tissue structures were calculated as the difference between follow-up and study inclusion values divided by the study inclusion value.

Statistical analysis

Descriptive statistics were calculated as frequencies and percentages for categorical variables and as central tendency (means) and dispersion (standard deviations) for continuous variables.

To assess the statistical significance of the categorical KR occurrences over time from study inclusion, a generalized estimating equation (GEE) method was used with KR as the response variable, follow-up time points, age, gender, and BMI as fixed factors, subject and error terms as random factors. To test the variation through time of the other continuous variables, an MMRM was used with the selected variable as response variable, follow-up time points, age, gender and BMI as fixed factors, and subject and error terms as random factors. The selected continuous variable value at study inclusion was also used as covariate. The within-patient covariance matrix was assumed to be unstructured.

Associations between IPFP characteristics at inclusion and the clinical and structural outcomes were evaluated using a multivariable analysis of covariance (ANCOVA). Selected continuous variables served as the response, IPFP characteristics at study inclusion as well as age, gender, and BMI at inclusion were used as covariates. For WOMAC scores, the intake of analgesic medications at the time of measure (follow-up) was also used as a covariate.

The association between the occurrence of a KR over time and IPFP signal intensities at inclusion was calculated for statistical relevance using an adjusted logistic regression. The occurrence of KR at selected follow-up times was the response variable, with IPFP characteristics at study inclusion, as well as age, gender at study inclusion, and BMI, WOMAC pain score, medial BML, and intake of analgesic medications at the study visit follow-up time as covariates.

All statistical analyses were performed using SPSS (IBM SPSS Statistics 26.0, IL, USA). Statistical tests were two-sided, with a *p*-value ≤ 0.05 considered statistically significant. As this was an exploratory study design, the statistical level of significance was not corrected for multiple comparisons.

Results

Demographic, clinical, and knee structure characteristics at study inclusion (Table 1)

Most knees were from female participants, and most were slightly overweight (>27 kg/m²). WOMAC pain and radiological scores indicated moderate levels of knee OA. For the IPFP volume/area, the hypointense signal comprises the largest portion vis à vis the hyperintense signal.

Changes in clinical and knee structure characteristics over time (12-96 months)

As shown in Table 2, the incidence of KR increased progressively over time, with 17.83% of knees requiring arthroplasty by 96-month follow-up. WOMAC scores showed a slight but consistent reduction in symptoms over time. Knee structure data revealed a progressive loss in cartilage volume and increased effusion volume, while BML volume exhibited only minimal changes. Regarding the IPFP, both global and hypointense signal volumes slightly decreased over time, whereas hyperintense signal volumes steadily increased, reaching 46.92% at 96 months. Similar trends were observed for the areas (maximal and hypo- and hyperintensity signals).

Association between clinical, knee structure, and IPFP characteristics at study inclusion

Cross-sectional data (Table 3) revealed significant positive associations between all IPFP morphology measures

Table 1 Demographic, clinical and knee structure characteristics of knees at study inclusion.

	(n=1075)
Age, years	61.98 (9.10)
Female	659 (61.30)
Target knee, Right	512 (47.63)
Body mass index, kg/m²	30.31 (4.98)
Body mass index, ≥ 27 kg/m²	781 (72.79)
WOMAC^a	
Total, 0-96	24.59 (18.17)
Pain, 0-20	5.34 (4.06)
Joint space width, mm	(n=940)
	3.83 (1.59)
Cartilage volume, mm³	(n=923)
Global knee	9,733.51 (2,731.13)
Medial compartment ^b	4,649.91 (1,563.48)
Bone marrow lesion volume, %	(n=926)
Global knee	1.63 (3.52)
Medial compartment	2.57 (5.53)
Effusion volume, mL	(n=936)
	13.59 (12.66)
Infrapatellar fat pad morphologies	(n=1,057)
Global volume, cm ³	24.91 (6.29)
Hypointense volume, cm ³	22.28 (5.80)
Hyperintense volume, cm ³	2.60 (0.87)
Maximal area, cm ²	6.24 (1.14)
Hypointense area, cm ²	5.48 (1.11)
Hyperintense area, cm ²	0.76 (0.42)

Data are mean and standard deviation or number of knees (n) or percentage (%)

^a WOMAC questionnaire was self-administered: higher WOMAC scores indicate more symptoms and greater functional impairment

^b Medial compartment: sum of medial condyle and medial plateau

n, number of cases; WOMAC, Western Ontario and McMaster Universities Osteoarthritis Index

and cartilage volume (both global knee and medial compartment; $p \leq 0.001$). Associations were also observed between the effusion volume with IPFP global volume, hyperintense volume, and hyperintense area ($p \leq 0.01$).

For BMLs (global knee and medial compartment), significant negative associations were found with IPFP global volume ($p \leq 0.004$), hypointense volume ($p \leq 0.002$) and area ($p \leq 0.001$), while a positive association was identified with the hyperintense area ($p \leq 0.03$).

No significant associations were found between clinical symptoms (WOMAC total and pain scores) and IPFP morphologies.

From a cross-sectional point of view, these data suggest that while IPFP morphology at inclusion is

predictive of knee structural changes, it does not appear to correlate with disease symptoms.

Association between longitudinal changes in clinical and knee structural characteristics and IPFP morphologies

The longitudinal data (Table 4) again showed no significant association between changes in disease symptoms over time and IPFP morphologies at study inclusion. However, significant associations were identified between longitudinal changes in structural characteristics and the IPFP morphologies at study inclusion. Key findings include the following. i) Cartilage volume. A negative association was observed between changes in

Table 2 Changes up to 96 months in clinical and knee structure characteristics

	12 months	24 months	48 months	96 months	<i>p</i> -value ^c
Knee replacement, n (%) – cumulative	(<i>n</i> =1075)	(<i>n</i> =858)	(<i>n</i> =858)	(<i>n</i> =858)	
	11 (1.02)	24 (2.80)	69 (8.04)	153 (17.83)	≤0.001
WOMAC^a, Δ	(<i>n</i> =1075)	(<i>n</i> =923)	(<i>n</i> =908)	(<i>n</i> =822)	
Total, 0-96	-2.18 (14.39)	-2.91 (15.71)	-3.84 (17.25)	-4.79 (18.68)	≤0.001
Pain, 0-20	-0.69 (3.28)	-0.84 (3.69)	-1.05 (4.06)	-1.37 (4.44)	≤0.001
Cartilage volume, Δ%	(<i>n</i> =866)	(<i>n</i> =771)	(<i>n</i> =649)	(<i>n</i> =368)	
Global knee	-2.40 (3.50)	-3.97 (4.19)	-5.40 (4.53)	-10.98 (9.92)	≤0.001
Medial compartment ^b	-2.67 (4.71)	-4.25 (5.48)	-5.62 (6.19)	-13.16 (13.38)	≤0.001
BML volume, Δ%	(<i>n</i> =866)	(<i>n</i> =774)	(<i>n</i> =651)	(<i>n</i> =409)	
Global knee	0.41 (2.32)	0.40 (2.26)	0.72 (2.45)	0.09 (1.81)	≤0.001
Medial compartment	0.41 (3.55)	0.34 (3.58)	0.70 (3.52)	-0.37 (3.00)	≤0.001
Effusion volume, Δ%	(<i>n</i> =872)	(<i>n</i> =776)	(<i>n</i> =657)	(<i>n</i> =413)	
	17.58 (87.82)	36.35 (156.95)	69.98 (182.09)	60.75 (180.79)	≤0.001
Infrapatellar fat pad, Δ%					
Volume					
Global	(<i>n</i> =883)	(<i>n</i> =778)	(<i>n</i> =678)	(<i>n</i> =435)	
	0.02 (7.83)	-2.20 (9.08)	-1.75 (7.76)	-5.22 (8.43)	≤0.001
Hypointense	(<i>n</i> =877)	(<i>n</i> =775)	(<i>n</i> =674)	(<i>n</i> =420)	
	0.01 (8.22)	-2.68 (9.71)	-2.55 (8.39)	-7.46 (8.55)	≤0.001
Hyperintense	(<i>n</i> =877)	(<i>n</i> =775)	(<i>n</i> =674)	(<i>n</i> =420)	
	2.59 (24.61)	6.03 (33.39)	10.16 (34.24)	21.10 (46.92)	≤0.001
Area					
Maximal	(<i>n</i> =879)	(<i>n</i> =778)	(<i>n</i> =678)	(<i>n</i> =435)	
	0.30 (6.76)	-1.15 (9.00)	-0.92 (8.57)	-3.10 (7.58)	≤0.001
Hypointense	(<i>n</i> =856)	(<i>n</i> =778)	(<i>n</i> =659)	(<i>n</i> =426)	
	0.21 (16.09)	-1.64 (11.38)	-2.03 (16.96)	-4.54 (10.24)	≤0.001
Hyperintense	(<i>n</i> =859)	(<i>n</i> =778)	(<i>n</i> =661)	(<i>n</i> =426)	
	8.32 (51.14)	17.46 (71.10)	19.04 (74.89)	26.37 (90.32)	≤0.001

Data are mean (standard deviation); Δ, difference between visit values and study inclusion value; Δ%, relative difference (Δ divided by study inclusion value)

^a WOMAC questionnaire was self-administered. Absolute changes in WOMAC scores: <0=improvement; 0=stable; >0=worsening

^b Medial compartment: sum of medial condyle and medial plateau

^c To assess the statistical significance of KR occurrences over time from study inclusion, a GEE method was used with KR as the response variable, follow-up time points, age, gender, and BMI as fixed factors, and subject and error terms as random factors. The *p*-values in bold indicate statistical significance (*p*≤0.05) BML, bone marrow lesion; GEE, generalized estimating equation; KR, knee replacement; n, number of knees; WOMAC, Western Ontario and McMaster Universities Osteoarthritis Index

the medial compartment and hypointense volume at 48 and 96 months (*p*≤0.04) and between changes in both global knee and medial compartment cartilage volume with hyperintense volume at 48 months (*p*≤0.03). ii) BML volume. A positive association was identified between changes in BML volume in the medial compartment and IPFP global volume at 48 months (*p*=0.05) and between changes in both the global knee and medial compartment BML volume with the hyperintense area at 12 months (*p*≤0.04). iii) Synovial effusion volume. A positive association was observed between synovial effusion volume and hypointense volume at 48 months (*p*=0.05), while a negative association was found with hyperintense volume at 96 months (*p*=0.04).

Further analysis of joint structural changes and IPFP morphology changes over time revealed a strong association between the effusion volume and the hyperintense

volume at all times (*p*≤0.02) and between the effusion volume and hypointense area at 12, 48, and 96 months (*p*≤0.02) (data not shown).

Association between cumulative KR over time and IPFP morphologies

Data in Table 5 show a statistically significant negative association between cumulative KR over time and IPFP size (below the median) and global and hypointense volume, and maximal area at 96 months (*p*=0.05), with a positive association for the hyperintense global volume at 24 months (*p*=0.02).

These results suggest a consistent reduction in the cumulative incidence of KR at 96 months for participants with smaller IPFP (volume/area) at inclusion.

Table 3 Association between clinical, knee structure and infrapatellar fat pad characteristics at study inclusion

	<i>n</i>	Global Volume	Hypointense Volume	Hyperintense Volume
		β (95% CI) <i>p</i> -value ^c		
WOMAC^a	1052			
Total, 0-96		0.04 (-0.21;0.29) 0.75	0.04 (-0.23;0.31) 0.78	0.44 (-0.97;1.86) 0.54
Pain, 0-20		0.01 (-0.04;0.07) 0.66	0.01 (-0.05;0.07) 0.70	0.12 (-0.20;0.44) 0.46
Cartilage volume	920			
Global knee		0.17 (0.14;0.20) ≤ 0.001	0.17 (0.13;0.20) ≤ 0.001	0.77 (0.58;0.96) ≤ 0.001
Medial compartment ^b		0.08 (0.07;0.10) ≤ 0.001	0.08 (0.06;0.10) ≤ 0.001	0.38 (0.27;0.50) ≤ 0.001
Bone marrow lesion volume	922			
Global knee		-0.09 (-0.14;-0.03) 0.001	-0.10 (-0.16;-0.05) ≤ 0.001	0.08 (-0.23;0.39) 0.61
Medial compartment		-0.13 (-0.21;-0.04) 0.004	-0.15 (-0.24;-0.05) 0.002	0.11 (-0.38;0.61) 0.65
Effusion volume, mL	931			
		0.03 (0.01;0.05) 0.01	0.16 (-0.05;0.37) 0.13	0.40 (0.29;0.51) ≤ 0.001
		Maximal Area	Hypointense Area	Hyperintense Area
	<i>n</i>	β (95% CI) <i>p</i> -value		
WOMAC	1052			
Total, 0-96		9.70 (-2.07;21.48) 0.11	8.60 (-2.07;21.48) 0.11	3.03 (-22.63;28.70) 0.82
Pain, 0-20		1.81 (-0.87;4.49) 0.19	1.67 (-0.94;4.28) 0.21	0.24 (-5.61;6.08) 0.94
Cartilage volume	920			
Global knee		6.59 (5.06;8.13) ≤ 0.001	4.80 (3.21;6.40) ≤ 0.001	17.23 (12.65;21.81) ≤ 0.001
Medial compartment		3.15 (2.21;4.09) ≤ 0.001	2.31 (1.34;3.28) ≤ 0.001	8.10 (5.30;10.90) ≤ 0.001
Bone marrow lesion volume	922			
Global knee		-1.49 (-4.04;1.06) 0.25	-2.76 (-5.36;-0.16) 0.04	10.20 (2.68;17.71) 0.01
Medial compartment		-2.53 (-6.56;1.49) 0.22	-4.23 (-8.33;-0.13) 0.04	13.40 (1.51;25.30) 0.03
Effusion volume, mL	931			
		0.36 (-0.55;1.27) 0.44	-5.66 (-14.95;3.63) 0.23	7.91 (5.26;10.56) ≤ 0.001

^a WOMAC questionnaire was self-administered

^b Medial compartment: sum of medial condyle and medial plateau

^c Each IPFP characteristic at inclusion was assessed for a relationship with the clinical and structural outcomes also at inclusion. The statistical relevance of such associations was calculated with a multivariable ANCOVA model with age, gender, and BMI values at inclusion as covariates. Negative β values indicate a negative impact on the variable response. The *p*-values in bold indicate statistical significance ($p \leq 0.05$)

ANCOVA, analysis of covariance; β , beta; BMI, body mass index; CI, confidence interval; IPFP, infrapatellar fat pad; *n*, number of knees; WOMAC, Western Ontario and McMaster Universities Osteoarthritis Index

Discussion

This exploratory work used the longest knee OA observational study currently available to evaluate the role of IPFP morphologies in predicting OA symptoms, knee structural changes, and outcomes. Assessments of IPFP were performed using MRI, enhanced by an improved software derived from our previously described fully automated neuron-driven technology [20]. The objective was to facilitate comparisons of IPFP volumes, areas, and signal intensities, all obtained from the same MRI acquisition, allowing for a simultaneous evaluation of various IPFP morphologies. This approach enabled a direct comparison of their predictive value for knee OA.

Our longitudinal findings indicate that global IPFP and signal volume, rather than area, may have better predictability values regarding disease progression for OA-related knee structural changes and the outcome, KR. In cross-sectional analyses, we observed associations between IPFP volume and area morphologies. Additionally, a comparison of signal morphologies revealed that both

hypointense and hyperintense signal intensities - volumes and areas in cross-sectional analysis and primarily volume in the longitudinal one - were highly valuable predictive factors. Hence, both signal intensities correlated with cartilage volume loss, increased BML, and higher effusion volume, all indicators of OA knee structural changes.

Among the IPFP morphologies, the hypointense component comprises the largest portion of the IPFP volume and area compared to the hyperintense signal (Table 1). Over time, global and hypointense signal volumes and areas decreased slightly, while hyperintense components showed a pronounced and consistent increase, suggesting an increase in inflammation/synovitis alongside OA severity progression [23, 37–39]. Further supporting the interaction between IPFP and synovium is the positive association between the effusion volume and hyperintense signal volume and area in cross-sectional analyses. This suggests that both tissues may act together to sustain joint inflammation [40, 41]. However, the longitudinal analyses showing a positive association of the hypointense

Table 4 Association between over-time changes^a in clinical and knee structure characteristics and infrapatellar fat pad morphologies at study inclusion^a

		12 months	24 months	48 months	96 months
		β (95% CI) <i>p</i> -value ^b			
		(<i>n</i> =860)	(<i>n</i> =766)	(<i>n</i> =644)	(<i>n</i> =363)
Global volume	WOMAC^c, Δ				
	Total, 0-96	-0.07 (-0.28;0.14) 0.51	-0.16 (-0.41;0.09) 0.21	-0.15 (-0.42;0.12) 0.29	-0.06 (-0.38;0.27) 0.73
	Pain, 0-20	-0.04 (-0.08;0.01) 0.14	-0.01 (-0.07;0.05) 0.69	-0.05 (-0.11;0.02) 0.16	-0.03 (-0.10;0.05) 0.48
	Cartilage volume, $\Delta\%$				
	Global knee	0.002 (-0.05;0.06) 0.93	0.01 (-0.06;0.08) 0.78	-0.04 (-0.12;0.04) 0.32	-0.06 (-0.31;0.19) 0.64
	Medial compartment ^d	-0.02 (-0.09;0.06) 0.62	0.02 (-0.07;0.11) 0.67	-0.10 (-0.21;0.01) 0.09	-0.18 (-0.51;0.15) 0.29
	Bone marrow lesion volume, $\Delta\%$				
	Global knee	0.01 (-0.02;0.05) 0.44	0.03 (-0.01;0.07) 0.14	0.03 (-0.01;0.08) 0.17	0.01 (-0.04;0.05) 0.72
	Medial compartment	0.03 (-0.03;0.09) 0.31	0.05 (-0.01;0.12) 0.08	0.07 (0.00;0.13) 0.05	0.03 (-0.04;0.11) 0.33
Effusion volume, $\Delta\%$	-0.52 (-1.95;0.90) 0.47	0.44 (-2.77;3.14) 0.75	2.30 (-1.01;5.62) 0.17	-3.52 (-7.78;0.74) 0.11	
Hypointense volume	WOMAC, Δ				
	Total, 0-96	-0.09 (-0.31;0.12) 0.39	-0.18 (-0.42;0.06) 0.15	-0.16 (-0.41;0.10) 0.23	0.02 (-0.28;0.32) 0.90
	Pain, 0-20	-0.04 (-0.09;0.01) 0.11	-0.01 (-0.07;0.04) 0.63	-0.04 (-0.10;0.02) 0.15	-0.01 (-0.07;0.06) 0.87
	Cartilage volume, $\Delta\%$				
	Global knee	-0.002 (-0.07;0.06) 0.95	-0.02 (-0.06;0.10) 0.63	-0.02 (-0.11;0.07) 0.62	-0.26 (-0.53;0.02) 0.07
	Medial compartment	-0.04 (-0.12;0.05) 0.37	-0.01 (-0.11;0.10) 0.89	-0.13 (-0.25;-0.004) 0.04	-0.48 (-0.83;-1.12) 0.01
	Bone marrow lesion volume, $\Delta\%$				
	Global knee	-0.001 (-0.04;0.04) 0.96	0.01 (-0.03;0.05) 0.73	0.20 (-0.03;0.07) 0.40	-0.003 (-0.04;0.03) 0.88
	Medial compartment	0.004 (-0.05;0.06) 0.89	0.02 (-0.05;0.08) 0.62	0.05 (-0.02;0.12) 0.13	0.02 (-0.03;0.07) 0.47
Effusion volume, $\Delta\%$	-0.34 (-1.82;1.15) 0.66	-1.08 (-1.76;3.92) 0.45	3.36 (-0.06;6.78) 0.05	-2.66 (-7.11;1.80) 0.24	
Hyperintense volume	WOMAC, Δ				
	Total, 0-96	0.41 (-0.77;1.59) 0.50	-0.44 (-1.84;0.97) 0.54	0.49 (-1.07;2.05) 0.54	0.12 (-1.72;1.95) 0.90
	Pain, 0-20	-0.10 (-0.36;0.17) 0.49	-0.06 (-0.38;0.27) 0.74	-0.02 (-0.38;0.35) 0.93	-0.06 (-0.49;0.37) 0.78
	Cartilage volume, $\Delta\%$				
	Global knee	-0.12 (-0.45;0.20) 0.46	-0.32 (-0.73;0.10) 0.13	-0.53 (-0.99;-0.06) 0.03	0.12 (-1.26;1.50) 0.87
	Medial compartment	-0.42 (-0.86;0.01) 0.06	-0.51 (-1.05;0.02) 0.06	-1.08 (-1.72;-0.45) 0.001	-0.55 (-2.39;1.30) 0.56
	Bone marrow lesion volume, $\Delta\%$				
	Global knee	-0.08 (-0.30;0.13) 0.45	-0.02 (-0.25;0.20) 0.86	0.04 (-0.22;0.29) 0.79	0.04 (-0.20;0.27) 0.76
	Medial compartment	-0.01 (-0.34;0.33) 0.97	0.03 (-0.33;0.39) 0.87	0.12 (-0.25;0.49) 0.53	0.04 (-0.35;0.43) 0.85
Effusion volume, $\Delta\%$	-0.58 (-8.77;7.61) 0.89	-4.36 (-19.92;11.21) 0.58	-5.61 (-24.61;13.39) 0.56	-24.80 (-48.27;-1.32) 0.04	
Maximal area	WOMAC, Δ				
	Total, 0-96	-6.36 (-16.54;3.82) 0.22	-11.52 (-22.78;0.53) 0.06	-11.52 (-24.25;1.21) 0.08	-4.76 (-20.02;10.50) 0.54
	Pain, 0-20	-2.08 (-4.40;0.25) 0.08	-1.45 (-4.19;1.28) 0.30	-2.80 (-5.79;0.18) 0.07	-1.19 (-4.71;2.33) 0.51
	Cartilage volume, $\Delta\%$				
	Global knee	0.73 (-1.91;3.37) 0.59	1.51 (-1.88;4.90) 0.38	0.55 (-3.30;4.40) 0.78	3.72 (-8.39;15.83) 0.55
	Medial compartment	0.48 (-3.08;4.04) 0.79	3.32 (-1.09;7.73) 0.14	-1.07 (-6.36;4.22) 0.69	-0.51 (-16.75;15.74) 0.95
	Bone marrow lesion volume, $\Delta\%$				
	Global knee	-0.06 (-1.86;1.71) 0.95	0.72 (-1.13;2.57) 0.45	0.36 (-1.77;2.49) 0.74	-0.05 (-2.11;2.02) 0.96
	Medial compartment	-0.30 (-3.01;2.41) 0.83	1.54 (-1.39;4.48) 0.30	1.57 (-1.51;4.64) 0.32	1.30 (-2.11;4.70) 0.45
Effusion volume, $\Delta\%$	-16.44 (-83.30;50.43) 0.63	8.10 (-120.34;136.55) 0.90	138.71 (-19.43;296.85) 0.09	-68.22 (-274.54;138.11) 0.52	
Hypointense area	WOMAC, Δ				
	Total, 0-96	-2.16 (-11.27;6.95) 0.64	-2.97 (-13.04;7.10) 0.56	-4.18 (-14.98;6.63) 0.45	4.88 (-8.44;18.20) 0.47
	Pain, 0-20	-0.97 (-3.01;1.06) 0.35	-0.20 (-2.52;2.13) 0.87	-1.05 (-3.56;1.45) 0.41	1.16 (-1.83;4.15) 0.45
	Cartilage volume, $\Delta\%$				
	Global knee	0.50 (-2.27;3.27) 0.72	2.12 (-1.40;5.64) 0.24	1.82 (-2.18;5.82) 0.37	-3.01 (-15.45;9.43) 0.63
	Medial compartment	-0.09 (-3.78;3.59) 0.96	2.90 (-1.60;7.41) 0.21	-1.16 (-6.59;4.27) 0.67	-7.94 (-24.03;8.15) 0.33
	Bone marrow lesion volume, $\Delta\%$				
	Global knee	0.01 (-1.72;1.73) 0.10	0.39 (-1.37;2.14) 0.67	0.18 (-1.94;2.30) 0.87	-0.21 (-1.93;1.51) 0.81
	Medial compartment	-0.16 (-2.79;2.47) 0.91	0.82 (-1.91;3.55) 0.56	1.41 (-1.63;4.45) 0.36	1.33 (-1.16;3.82) 0.29
Effusion volume, $\Delta\%$	-16.85 (-83.19;49.49) 0.62	8.14 (-119.26;135.54) 0.90	137.45 (-17.19;292.09) 0.08	-70.35 (-273.93;133.22) 0.50	
Hyperintense area	WOMAC, Δ				
	Total, 0-96	-6.55 (-28.48;15.39) 0.56	-20.82 (-44.63;2.99) 0.09	-5.16 (-31.55;21.23) 0.70	-0.69 (-45.66;44.28) 0.98
	Pain, 0-20	-2.77 (-7.77;2.24) 0.28	-2.50 (-8.12;3.12) 0.38	-1.30 (-7.52;4.92) 0.68	-1.13 (-11.59;9.32) 0.83
	Cartilage volume, $\Delta\%$				
	Global knee	0.16 (-7.64;7.96) 0.97	-1.72 (-14.42;4.99) 0.34	-7.54 (-18.87;3.79) 0.19	15.09 (-18.79;48.97) 0.38
	Medial compartment	-2.39 (-12.90;8.12) 0.66	-7.10 (-19.73;5.53) 0.27	-12.01 (-27.60;3.57) 0.13	3.04 (-42.42;48.49) 0.90
	Bone marrow lesion volume, $\Delta\%$				
	Global knee	-5.35 (-10.55;-0.15) 0.04	-3.54 (-8.82;1.74) 0.19	0.45 (-6.72;5.82) 0.89	-0.49 (-6.44;5.46) 0.87
	Medial compartment	-8.77 (-16.74;-0.80) 0.03	-6.06 (-14.45;2.32) 0.16	-2.43 (-11.50;6.64) 0.60	-5.87 (-15.66;3.92) 0.24
Effusion volume, $\Delta\%$	-105.43 (-302.48;91.62) 0.29	-141.18 (-507.72;225.35) 0.45	-175.64 (-641.99;290.71) 0.46	-90.34 (-682.77;502.09) 0.77	

A. absolute difference; $\Delta\%$, relative difference (Δ divided by study inclusion value)

^a Study inclusion characteristic can be found in Table 1, and follow-up characteristics can be found in Table 2

^b Each IPPF characteristic at inclusion was assessed for a relationship with the clinical and structural outcomes at each time point. The statistical relevance of such associations was calculated with a multivariable ANCOVA model with age, gender, and BMI values at inclusion as covariates. For WOMAC scores specifically, the intake of analgesic medications at each time of measure (follow-up) was also used as a covariate. Negative β values indicate a negative impact on the variable response. The *p*-values in bold indicate statistical significance (*p*≤0.05)

^c WOMAC questionnaire was self-administered

^d Medial compartment: sum of medial condyle and medial plateau

ANCOVA, analysis of covariance; β , beta; BMI, body mass index; CI, confidence interval; IPPF, infrapatellar fat pad; *n*, number of knees; WOMAC, Western Ontario and McMaster Universities Osteoarthritis Index

IPFP volume with the effusion volume at 48 months and the negative association with hyperintense volume at 96 months are intriguing, and no definitive conclusions could be drawn. Yet, the strong positive correlation between changes in hyperintense volume and effusion volume over the entire follow-up period underscores the role of these alterations and joint inflammation. These findings build upon prior research [23] and reinforce the association of effusion synovitis and IPFP signal intensity with an elevated risk of accelerated knee OA [42].

The cross-sectional data revealing a significant positive association between all IPFP morphologies (volumes and areas) and cartilage volume likely reflects increased cartilage volume in knees with larger IPFP and, therefore, greater hyperintense signal volume, probably related to cartilage edema, which MRI commonly detects in early OA stages [43, 44]. Similar associations were reported in a community-based elderly cohort [11, 12, 45].

In the longitudinal analysis, both hypointense and hyperintense IPFP volumes, but not areas, were associated with greater long-term cartilage volume loss, with significant associations observed at 48 and/or 96 months, an expected outcome in knees with mild OA. Notably, a trend was seen for an association with cartilage volume in the medial compartment at 12 and 24 months for hyperintense volume, suggesting an early cartilage volume loss, reinforcing the link between joint inflammation and cartilage degradation [8, 27, 38, 42]. Other shorter longitudinal (48 months or less) works that quantified IPFP volume signal intensity in knee OA have similarly reported associations with cartilage volume loss over time [17, 22, 23]. In contrast, our data regarding IPFP surface and signal areas indicating no association with long-term cartilage loss diverge from other studies [10–12, 17], as well as with the suggestion of a protective effect of larger IPFP on knee cartilage [26]. These differences may result from methodological differences, such as the differences between the studies cohorts and duration, the methods used for the assessment of structural changes, including IPFP morphologies, and the use of ordinal and not continuous scoring methods with any real cut-off to differentiate the hyperintense and hypointense signal.

On cross-sectional analyses, our study shows a negative association between BML volume and IPFP global volume and hypointense volume and area, but a positive one with the hyperintense area reinforces the role of inflammation in promoting subchondral bone changes.[41, 46] This concurs with data from other cross-sectional works [2, 11, 17] using similar symptomatic knee OA patients cohorts, which reported that IPFP hyperintensity signal volume was positively associated with increased BML. However, it contrasts with a previous report [11], where

a positive relationship was observed between the hypointense signal area and BML. There could be several possible explanations for the latter finding. First, as mentioned above, the two studies had different study designs and selected variables. Second, the use of a semi-quantitative method rather than a fully automated algorithm to assess IPFP morphologies, as in the present study, may have also contributed to differences in findings.

The longitudinal findings on BML demonstrated that IPFP volume morphologies were superior predictors of disease progression in contrast to the area, except for a negative association between hyperintense area and BML found only at 12 months. Hence, IPFP global volume at inclusion predicted the increase in BML size over time, with a significant positive association at 48 months and a trend at 24 months. Given this structure's relatively small size at inclusion, a finding somewhat expected in early OA, the significant association at 48 months may reflect the slow BML progression in our study population with mid-moderate OA [47]. The reduction in BML size found at 96 months could possibly be explained by the fact that, over time, BMLs may undergo some reduction in size with the occurrence of chronic sclerosis (scar tissue), which is expected in chronic bone lesions [47]. The findings are new and interesting, as very few studies have followed the evolution of BMLs in knee OA over such an extended period (96 months). Again, the IPFP area data differ from other studies reporting a positive association between BML and IPFP hypointense or hyperintense signal area [11, 12, 17] for reasons already discussed.

Symptom assessment using a standardized continuous scale (WOMAC scale) revealed a small but gradual decrease in symptom severity over time while structural changes increased, consistent with previous reports [48–51]. Cross-sectional analysis showed no association between IPFP morphologies and symptom severity at inclusion, aligning with findings from a comprehensive case-control study conducted on the OAI progression cohort [15] where IPFP morphologies were manually assessed, and with another study [21] that used semi-automatic contouring to measure IPFP maximal area and signal intensity in patients with symptomatic knee OA. However, other studies have reported significant positive associations between the IPFP area and symptom severity [12, 17]. The discrepancies in findings between those and our study could stem from several factors: some of these studies included participants from an elderly population rather than individuals with symptomatic knee OA as in our study, symptom definitions were not clinically relevant according to the investigators, and the analyses relied on using non-continuous variables. Furthermore, only manually assessed IPFP area was considered, limiting direct comparisons with other IPFP morphologies. Lastly, data analyses in these studies did not adjust

Table 5 Association between overtime cumulative knee replacements and infrapatellar fat pad morphologies at study inclusion^a

		12 months	24 months	48 months	96 months
		β (95% CI) <i>p</i> -value ^b			
Knee replacement ^c		(<i>n</i> =11)	(<i>n</i> =24)	(<i>n</i> =89)	(<i>n</i> =153)
Global volume	Global	0.18 (-0.32;0.68) 0.49	0.04 (-0.10;0.19) 0.58	-0.02 (-0.10;0.06) 0.61	-0.01 (-0.06;0.05) 0.85
	< median ^d	N/C	0.08 (-0.22;0.38) 0.60	-0.11 (-0.26;0.05) 0.18	-0.11 (-0.22;-0.01) 0.04
	≥ median	0.10 (-0.49;0.68) 0.75	0.02 (-0.23;0.26) 0.90	-0.04 (-0.16;0.08) 0.55	0.02 (-0.06;0.10) 0.56
Hypointense volume	Global	0.19 (-0.34;0.72) 0.47	0.01 (-0.14;0.17) 0.89	-0.03 (-0.11;0.05) 0.47	-0.01 (-0.07;0.04) 0.66
	< median	N/C	0.01 (-0.30;0.32) 0.94	-0.16 (-0.32;0.01) 0.06	-0.14 (-0.26;-0.03) 0.02
	≥ median	0.11 (-0.51;0.74) 0.73	-0.03 (-0.31;0.25) 0.82	-0.04 (-0.17;0.09) 0.54	0.05 (-0.04;0.13) 0.31
Hyperintense volume	Global	0.34 (-1.97;2.65) 0.77	0.83 (0.11;1.55) 0.02	0.18 (-0.22;0.58) 0.37	0.18 (-0.10;0.46) 0.20
	< median	N/C	0.89 (-1.96;3.74) 0.54	0.33 (-0.92;1.59) 0.61	0.57 (-0.25;1.39) 0.17
	≥ median	0.05 (-2.73;2.83) 0.97	0.95 (-0.10;2.00) 0.08	0.04 (-0.63;0.70) 0.91	0.16 (-0.31;0.64) 0.50
Maximal area	Global	8.20 (-13.83;30.22) 0.47	-0.22 (-6.93;6.49) 0.95	-2.49 (-6.01;1.03) 0.17	-1.71 (-4.09;0.66) 0.16
	< median	N/C	-0.37 (-14.69;13.94) 0.96	-5.19 (-12.79;2.42) 0.18	-5.32 (-10.64;-0.01) 0.05
	≥ median	7.00 (-17.34;31.35) 0.57	1.69 (-10.78;14.16) 0.79	-0.35 (-6.68;5.99) 0.91	1.76 (-2.36;5.87) 0.40
Hypointense area	Global	9.15 (-15.33;33.62) 0.46	-0.87 (-7.81;6.06) 0.81	-2.42 (-6.05;1.21) 0.19	1.88 (-4.33;0.57) 0.13
	< median	N/C	-1.30 (-15.33;12.73) 0.86	-5.87 (-13.50;1.76) 0.13	-5.04 (-10.37;0.29) 0.06
	≥ median	7.48 (-19.83;34.78) 0.59	-1.51 (-16.87;13.85) 0.85	-2.97 (-10.11;4.17) 0.42	2.21 (-2.24;6.66) 0.33
Hyperintense area	Global	2.43 (-60.30;65.16) 0.94	4.69 (-13.91;23.30) 0.62	-1.81 (-12.00;8.38) 0.73	0.53 (-6.34;7.41) 0.73
	< median	N/C	27.76 (-102.57;47.05) 0.47	4.71 (-28.57;38.00) 0.78	19.42 (-3.59;42.44) 0.10
	≥ median	28.30 (-140.24;83.64) 0.62	-20.46 (-57.68;16.77) 0.28	-4.83 (-24.44;14.77) 0.63	-3.98 (-17.49;9.54) 0.56

^a IPFP study inclusion characteristic values can be found in Table 1

^b Associations between IPFP characteristics at inclusion and occurrence of KR were calculated for statistical relevance using adjusted logistic regression with the occurrence of KR at the different time-point visits as the response variable, IPFP characteristics at inclusion as an independent variable and the following study inclusion variables: age, gender, BMI, intake of analgesic medications, WOMAC pain score and medial BML as covariates. Negative β values indicate a negative impact on the variable response. The *p*-values in bold indicate statistical significance (≤ 0.05)

^c Knee replacements are those occurring up to the date of the follow-up visit

^d Study inclusion median values of IPFP characteristics: volume: global: 24.0 cm³; hyperintense: 2.5 cm³; hypointense: 21.4 cm³; area: maximal: 6.1 cm²; hyperintense: 0.7 cm²; hypointense: 5.4 cm²

β , beta; BMI, body mass index; BML, bone marrow lesion; CI, confidence interval; IPFP, infrapatellar fat pad; KR, knee replacement; N/C, not computable; WOMAC, Western Ontario and McMaster Universities Osteoarthritis Index

for key confounding factors, such as analgesic use and BML size, to name a few, which could impact symptom levels.

Longitudinally, even when stratifying data (WOMAC pain < 7 \geq ; data not shown), no associations between IPFP morphologies and OA symptoms were observed. This finding aligns with two shorter-term (≤ 53 months) longitudinal studies on knee OA patients [14, 18] but differs from other studies [10, 26]. However, in the latter, only participants with heightened symptoms were exclusively selected, potentially skewing results. Moreover, the use of a low threshold (WOMAC pain score ≥ 1) to define symptomatic patients [10] raises further questions from a clinical perspective.

Finally, an important finding was the negative association of smaller IPFP (global and hypointense volumes and maximal area) at study inclusion with KR at 96 months, suggesting a potential protective effect against KR. Conversely, a greater hyperintense volume was associated with increased KR risk, albeit only at 24 months, confirming and expanding on findings from a nested case-control study (over 60 months) using OAI participants with severe knee OA [16]. The finding of reduced KR incidence in joints with smaller IPFP is interesting, considering the negative association of hypointense volume with cartilage

change (smaller IPFP means smaller cartilage loss), which should have lowered the risk for KR [50, 51].

While our findings provide valuable insights into IPFP morphologies as potential independent predictors for OA progression and KR, some limitations should be considered. Our exploratory study focused on the role of IPFP morphology as an independent risk factor for the progression and outcome of OA. In the future, it would be worthwhile to investigate other interesting markers using different study designs, such as machine learning. Our sample primarily consisted of individuals with mild to moderate knee OA, which might have impacted the timing of associations observed and could explain why significant associations were found in the latter follow-up period. Additionally, this study lacked data on other parameters, including cartilage defects and JSW in the association's analyses. However, for the JSW, this was because we used the OAI central reading data, which was available only until 48 months. When considering the potential relationship between joint effusion and synovitis, it is important to exercise caution, as this study did not conduct any contrast-enhanced assessments of the synovial membrane. A higher incidence of KR would have enhanced the statistical power, though OAI remains the largest cohort with such a long follow-up

period. Moreover, while our findings offer new insights into how IPFP morphologies may relate to disease outcomes, this study did not identify the most relevant IPFP morphological factors directly linking them to KR; further in-depth exploration is required. Since the overall intent of our work was to perform an exploratory study to probe potential relations between IPFP morphologies and symptomatic and structural knee OA changes over time, we did not adjust our *p*-values for multiple comparisons (multiplicity) as one should, for instance, for a clinical trial. Finally, while this technology is reproducible – being entirely computer-calculated and consistently yielding identical results for the same distribution – it is not possible to manually validate the signal intensities. The limitation arises because no visual approach can effectively separate voxels into two distinct classes based solely on their intensity.

Conclusions

This is the longest study to date and the first to directly compare the predictive value of different IPFP morphologies. It revealed that i) IPFP volume, including global and both hypointense and hyperintense signals, has better predictive value than area-based morphologies, and ii) smaller IPFP volume and area are associated with a reduced need for KR. These findings provide valuable insights into the comparative value of IPFP morphologies (volume and area) as predictive biomarkers for knee OA outcomes, which could help stratify knee OA patients.

Abbreviations

ANCOVA	analysis of covariance
BMI	body mass index
BMLs	bone marrow lesions
GEE	generalized estimating equation
IPFP	infrapatellar fat pad
JSW	joint space width
KR	knee replacement
MRI	magnetic resonance imaging
MMRM	mixed model for repeated measures
OA	osteoarthritis
STROBE	Strengthening the Reporting of Observation Studies in Epidemiology
OAI	Osteoarthritis Initiative
WOMAC	Western Ontario and McMaster Universities Osteoarthritis Index

Supplementary Information

The online version contains supplementary material available at <https://doi.org/10.1186/s13075-025-03513-y>.

Supplementary Material 1.

Acknowledgments

The authors would like to thank the Osteoarthritis Initiative (OAI) participants and the Coordinating Center for generating the OAI cohort's clinical and radiological data and making them publicly available. The OAI is a public-private partnership comprised of five contracts (N01-AR-2-2258; N01-AR-2-2259; N01-AR-2-2260; N01-AR-2-2261; N01-AR-2-2262) funded by the National Institutes of Health, a branch of the Department of Health and Human Services, and conducted by the OAI Study Investigators. Private funding partners

include Merck Research Laboratories, Novartis Pharmaceuticals Corporation, GlaxoSmithKline, and Pfizer Inc. Private sector funding for the OAI is managed by the National Institutes of Health Foundation. This manuscript was prepared using an OAI public use data set and does not necessarily reflect the opinions or views of the OAI investigators, the NIH, or the private funding partners. None of the authors are part of the OAI investigator team. A special thanks to ArthroLab Inc., Montreal, Canada, for providing the magnetic resonance imaging data and Santa Fiori for preparing the manuscript.

Authors' contributions

JPP is responsible for the overall content as the guarantor. JPP, MD, and JMP contributed to the study's conception and design. All authors (JPP, PP, FA, MD, JPR, JMP) were implicated in data curation, analysis, investigation, methodology, validation and visualization. PP generated the figure and first draft of the tables. All the authors (JPP, PP, FA, MD, JPR, JMP) were also involved in drafting the manuscript, and they all read and approved the final manuscript.

Funding

This work was supported in part by the Osteoarthritis Research Unit of the University of Montreal Hospital Research Centre and the Chair in Osteoarthritis from the University of Montreal. The funders had no role in study design, data collection and analysis, decision to publish, or manuscript preparation.

Data availability

Data from the Osteoarthritis Initiative cohort used in this study is publicly available (<https://data-archive.nimh.nih.gov/oai/>). The additional data used and analyzed for the current study are available from the corresponding author upon reasonable request, as long as the request is evaluated as scientifically relevant.

Declarations

Ethics approval and consent to participate

All Osteoarthritis Initiative (OAI) participants provided written informed consent for participation in the OAI. Ethics approval was obtained by each OAI clinical site (University of Maryland Baltimore Institutional Review Board, Ohio State University's Biomedical Sciences Institutional Review Board, University of Pittsburgh Institutional Review Board, and Memorial Hospital of Rhode Island Institutional Review Board) and the OAI Coordinating Center (Committee on Human Research at the University of California, San Francisco, CA, USA (47-00532)). All patients gave their written informed consent. The Institutional Ethics Committee Board of the University of Montreal Hospital Research Centre (48-9412, 20.321-YP) approved the project.

Consent for publication

Not applicable.

Competing interests

The authors declare no competing interests.

Author details

¹University of Montreal Hospital Research Centre (CRCHUM), Osteoarthritis Research Unit, 900 Saint-Denis, Room R11.412A, Montreal, Quebec H2X 0A9, Canada. ²StatSciences Inc, Notre-Dame de-l'Île-Perrot, Notre-Dame, Quebec, Canada.

Received: 2 December 2024 Accepted: 20 February 2025

Published online: 26 April 2025

References

1. Mobasheri A, Thudium CS, Bay-Jensen AC, Maleitcke T, Geissler S, Duda GN, et al. Biomarkers for osteoarthritis: Current status and future prospects. *Best Pract Res Clin Rheumatol*. 2023;37(2):101852.
2. Han W, Cai S, Liu Z, Jin X, Wang X, Antony B, et al. Infrapatellar fat pad in the knee: is local fat good or bad for knee osteoarthritis? *Arthritis Res Ther*. 2014;16(4):R145.
3. Martel-Pelletier J, Tardif G, Pelletier JP. An open debate on the morphological measurement methodologies of the infrapatellar fat pad to

- determine its association with the osteoarthritis process. *Curr Rheumatol Rep.* 2022;24(3):76–80.
4. Ushiyama T, Chano T, Inoue K, Matsusue Y. Cytokine production in the infrapatellar fat pad: another source of cytokines in knee synovial fluids. *Ann Rheum Dis.* 2003;62(2):108–12.
 5. Distel E, Cadoudal T, Durant S, Poignard A, Chevalier X, Benelli C. The infrapatellar fat pad in knee osteoarthritis: an important source of interleukin-6 and its soluble receptor. *Arthritis Rheum.* 2009;60(11):3374–7.
 6. Gierman LM, Wopereis S, van El B, Verheij ER, Werff-van der Vat BJ, Bastiaansen-Jenniskens YM, et al. Metabolic profiling reveals differences in concentrations of oxylipins and fatty acids secreted by the infrapatellar fat pad of donors with end-stage osteoarthritis and normal donors. *Arthritis Rheum.* 2013;65(10):2606–14.
 7. Conde J, Scoteca M, Lopez V, Abella V, Hermida M, Pino J, et al. Differential expression of adipokines in infrapatellar fat pad (IPFP) and synovium of osteoarthritis patients and healthy individuals. *Ann Rheum Dis.* 2014;73(3):631–3.
 8. Martel-Pelletier J, Paiement P, Pelletier JP. Magnetic resonance imaging assessments for knee segmentation and their use in combination with machine/deep learning as predictors of early osteoarthritis diagnosis and prognosis. *Ther Adv Musculoskelet Dis.* 2023; 15:1759720x231165560.
 9. Cai J, Xu J, Wang K, Zheng S, He F, Huan S, et al. Association between infrapatellar fat pad volume and knee structural changes in patients with knee osteoarthritis. *J Rheumatol.* 2015;42(10):1878–84.
 10. Pan F, Han W, Wang X, Liu Z, Jin X, Antony B, et al. A longitudinal study of the association between infrapatellar fat pad maximal area and changes in knee symptoms and structure in older adults. *Ann Rheum Dis.* 2015;74(10):1818–24.
 11. Han W, Aitken D, Zhu Z, Halliday A, Wang X, Antony B, et al. Hypointense signals in the infrapatellar fat pad assessed by magnetic resonance imaging are associated with knee symptoms and structure in older adults: a cohort study. *Arthritis Res Ther.* 2016;18(1):234.
 12. Han W, Aitken D, Zhu Z, Halliday A, Wang X, Antony B, et al. Signal intensity alteration in the infrapatellar fat pad at baseline for the prediction of knee symptoms and structure in older adults: a cohort study. *Ann Rheum Dis.* 2016;75(10):1783–8.
 13. Roemer FW, Jarraya M, Felson DT, Hayashi D, Crema MD, Loeuille D, et al. Magnetic resonance imaging of Hoffa's fat pad and relevance for osteoarthritis research: a narrative review. *Osteoarthritis Cartilage.* 2016;24(3):383–97.
 14. Schwaiger BJ, Mbapte Wamba J, Gersing AS, Nevitt MC, Facchetti L, McCulloch CE, et al. Hyperintense signal alteration in the suprapatellar fat pad on MRI is associated with degeneration of the patellofemoral joint over 48 months: data from the Osteoarthritis Initiative. *Skeletal Radiol.* 2018;47(3):329–39.
 15. Steidle-Kloc E, Culverer AG, Dorrenberg J, Wirth W, Ruhdorfer A, Eckstein F. Relationship between knee pain and infrapatellar fat pad morphology: A within- and between-person analysis from the Osteoarthritis Initiative. *Arthritis Care Res (Hoboken).* 2018;70(4):550–7.
 16. Wang K, Ding C, Hannon MJ, Chen Z, Kwok CK, Lynch J, et al. Signal intensity alteration within infrapatellar fat pad predicts knee replacement within 5 years: data from the Osteoarthritis Initiative. *Osteoarthritis Cartilage.* 2018;26(10):1345–50.
 17. Han W, Aitken D, Zheng S, Wluka AE, Zhu Z, Blizzard L, et al. Association between quantitatively measured infrapatellar fat pad high signal-intensity alteration and magnetic resonance imaging-assessed progression of knee osteoarthritis. *Arthritis Care Res (Hoboken).* 2019;71(5):638–46.
 18. Masaki T, Takahashi K, Hashimoto S, Ikuta F, Watanabe A, Kiuchi S, et al. Volume change in infrapatellar fat pad is associated not with obesity but with cartilage degeneration. *J Orthop Res.* 2019;37(3):593–600.
 19. Wang K, Ding C, Hannon MJ, Chen Z, Kwok CK, Hunter DJ. Quantitative signal intensity alteration in infrapatellar fat pad predicts incident radiographic osteoarthritis: The Osteoarthritis Initiative. *Arthritis Care Res (Hoboken).* 2019;71(1):30–8.
 20. Bonakdari H, Tardif G, Abram F, Pelletier JP, Martel-Pelletier J. Serum adipokines/related inflammatory factors and ratios as predictors of infrapatellar fat pad volume in osteoarthritis: Applying comprehensive machine learning approaches. *Sci Rep.* 2020;10(1):9993.
 21. He J, Ba H, Feng J, Peng C, Liao Y, Li L, et al. Increased signal intensity, not volume variation of infrapatellar fat pad in knee osteoarthritis: A cross-sectional study based on high-resolution magnetic resonance imaging. *J Orthop Surg (Hong Kong).* 2022;30(1):10225536221092216.
 22. Cen H, Yan Q, Meng T, Chen Z, Zhu J, Wang Y, et al. Quantitative infrapatellar fat pad signal intensity alteration as an imaging biomarker of knee osteoarthritis progression. *RMD Open.* 2023; 9(1).
 23. Ruan G, Lu S, Zhang Y, Zhu Z, Cao P, Wang X, et al. Quantitatively measured infrapatellar fat pad signal intensity alteration is associated with joint effusion-synovitis in knee osteoarthritis. *Curr Med Imaging.* 2024;20:e100323214543.
 24. Wang Z, Lu J, Li Z, Wang Y, Ge H, Zhang M, et al. Qualitative and quantitative measures in the infrapatellar fat pad in older adults: associations with knee pain, radiographic osteoarthritis, kinematics, and kinetics of the knee. *Acad Radiol.* 2024;31(8):3315–26.
 25. Cowan SM, Hart HF, Warden SJ, Crossley KM. Infrapatellar fat pad volume is greater in individuals with patellofemoral joint osteoarthritis and associated with pain. *Rheumatol Int.* 2015;35(8):1439–42.
 26. Teichtahl AJ, Wulidasari E, Brady SR, Wang Y, Wluka AE, Ding C, et al. A large infrapatellar fat pad protects against knee pain and lateral tibial cartilage volume loss. *Arthritis Res Ther.* 2015;17:318.
 27. Hill CL, Hunter DJ, Niu J, Clancy M, Guermazi A, Genant H, et al. Synovitis detected on magnetic resonance imaging and its relation to pain and cartilage loss in knee osteoarthritis. *Ann Rheum Dis.* 2007;66(12):1599–603.
 28. Roemer FW, Guermazi A, Zhang Y, Yang M, Hunter DJ, Crema MD, et al. Hoffa's fat pad: evaluation on unenhanced MR Images as a measure of patellofemoral synovitis in osteoarthritis. *AJR Am J Roentgenol.* 2009;192(6):1696–700.
 29. Dragoo JL, Johnson C, McConnell J. Evaluation and treatment of disorders of the infrapatellar fat pad. *Sports Med.* 2012;42(1):51–67.
 30. Chuckpaiwong B, Charles HC, Kraus VB, Guilak F, Nunley JA. Age-associated increases in the size of the infrapatellar fat pad in knee osteoarthritis as measured by 3T MRI. *J Orthop Res.* 2010;28(9):1149–54.
 31. von Elm E, Altman DG, Egger M, Pocock SJ, Gotsche PC, Vandenbroucke JP, et al. The strengthening of reporting of observational studies in epidemiology (STROBE) statement: guidelines for reporting observational studies. *Ann Intern Med.* 2007;147(8):573–7.
 32. Peterfy CG, Schneider E, Nevitt M. The osteoarthritis initiative: report on the design rationale for the magnetic resonance imaging protocol for the knee. *Osteoarthritis Cartilage.* 2008;16(12):1433–41.
 33. Bellamy N, Buchanan WW, Goldsmith CH, Campbell J, Stitt LW. Validation study of WOMAC: a health status instrument for measuring clinically important patient relevant outcomes to antirheumatic drug therapy in patients with osteoarthritis of the hip or knee. *J Rheumatol.* 1988;15:1833–40.
 34. Dodin P, Pelletier JP, Martel-Pelletier J, Abram F. Automatic human knee cartilage segmentation from 3D magnetic resonance images. *IEEE Trans Biomed Eng.* 2010;57(11):2699–711.
 35. Li W, Abram F, Pelletier JP, Raynauld JP, Dorais M, d'Anjou MA, et al. Fully automated system for the quantification of human osteoarthritic knee joint effusion volume using magnetic resonance imaging. *Arthritis Res Ther.* 2010;12(5):R173.
 36. Dodin P, Abram F, Pelletier J-P, Martel-Pelletier J. A fully automated system for quantification of knee bone marrow lesions using MRI and the osteoarthritis initiative cohort. *J Biomed Graph Comput.* 2013;3(1):51–65.
 37. Cao M, Ong MTY, Yung PSH, Tuan RS, Jiang Y. Role of synovial lymphatic function in osteoarthritis. *Osteoarthritis Cartilage.* 2022;30(9):1186–97.
 38. De Roover A, Escribano-Núñez A, Monteagudo S, Lories R. Fundamentals of osteoarthritis: Inflammatory mediators in osteoarthritis. *Osteoarthritis Cartilage.* 2023;31(10):1303–11.
 39. Zhao K, Ruan J, Nie L, Ye X, Li J. Effects of synovial macrophages in osteoarthritis. *Front Immunol.* 2023;14:1164137.
 40. Zhou S, Maleitzke T, Geissler S, Hildebrandt A, Fleckenstein FN, Niemann M, et al. Source and hub of inflammation: The infrapatellar fat pad and its interactions with articular tissues during knee osteoarthritis. *J Orthop Res.* 2022;40(7):1492–504.
 41. Li X, Chen W, Liu D, Chen P, Wang S, Li F, et al. Pathological progression of osteoarthritis: a perspective on subchondral bone. *Front Med.* 2024;18(2):237–57.
 42. Davis JE, Ward RJ, MacKay JW, Lu B, Price LL, McAlindon TE, et al. Effusion-synovitis and infrapatellar fat pad signal intensity alteration differentiate accelerated knee osteoarthritis. *Rheumatology (Oxford).* 2019;58(3):418–26.
 43. Raynauld JP, Martel-Pelletier J, Berthiaume MJ, Beaudoin G, Choquette D, Haraoui B, et al. Long term evaluation of disease progression through the

- quantitative magnetic resonance imaging of symptomatic knee osteoarthritis patients: correlation with clinical symptoms and radiographic changes. *Arthritis Res Ther*. 2006;8(1):R21.
44. Raynauld JP, Martel-Pelletier J, Berthiaume MJ, Abram F, Choquette D, Haraoui B, et al. Correlation between bone lesion changes and cartilage volume loss in patients with osteoarthritis of the knee as assessed by quantitative magnetic resonance imaging over a 24-month period. *Ann Rheum Dis*. 2008;67(5):683–8.
 45. Hall J, Laslett LL, Martel-Pelletier J, Pelletier JP, Abram F, Ding CH, et al. Change in knee structure and change in tibiofemoral joint space width: a five year longitudinal population-based study. *BMC Musculoskelet Disord*. 2016;17:25.
 46. Roelofs AJ, De Bari C. Osteoarthritis year in review 2023: Biology. *Osteoarthritis Cartilage*. 2024;32(2):148–58.
 47. Singh V, Oliashirazi A, Tan T, Fayyad A, Shahi A. Clinical and pathophysiologic significance of MRI identified bone marrow lesions associated with knee osteoarthritis. *Arch Bone Jt Surg*. 2019;7(3):211–9.
 48. Passey C, Kimko H, Nandy P, Kagan L. Osteoarthritis disease progression model using six year follow-up data from the osteoarthritis initiative. *J Clin Pharmacol*. 2015;55(3):269–78.
 49. Halilaj E, Le Y, Hicks JL, Hastie TJ, Delp SL. Modeling and predicting osteoarthritis progression: data from the osteoarthritis initiative. *Osteoarthritis Cartilage*. 2018;26(12):1643–50.
 50. Pelletier JP, Dorais M, Paiement P, Raynauld JP, Martel-Pelletier J. Risk factors associated with the occurrence of total knee arthroplasty in patients with knee osteoarthritis: a nested case-control study. *Ther Adv Musculoskelet Dis*. 2022; 14:1759720X221091359.
 51. Pelletier J-P, Paiement P, Dorais M, Raynauld J-P, Martel-Pelletier J. Risk factors for the long-term incidence and progression of knee osteoarthritis in older adults: role of nonsurgical injury. *Ther Adv Chronic Dis*. 2023;14:1–18.

Publisher's Note

Springer Nature remains neutral with regard to jurisdictional claims in published maps and institutional affiliations.